

AD-A242 880



2

PL-TR-91-2034

FRONT DETECTION WITH DOPPLER RADAR

Donald Hamann

ST Systems Corporation
109 Massachusetts Avenue
Lexington, MA 02173

15 February 1991

Scientific Report No. 3

APPROVED FOR PUBLIC RELEASE; DISTRIBUTION UNLIMITED



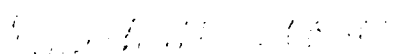
PHILLIPS LABORATORY
AIR FORCE SYSTEMS COMMAND
HANSCom AIR FORCE BASE, MASSACHUSETTS 01731-5000

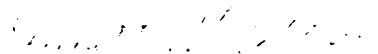
91-16441



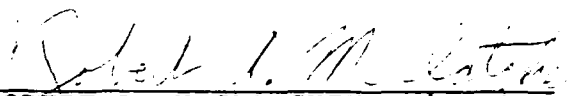
01 1125 065

"This technical report has been reviewed and is approved for publication"


KENNETH M. GLOVER
Contract Manager


KENNETH M. GLOVER, Chief
Ground Based Remote Sensing Branch
Atmospheric Sciences Division

FOR THE COMMANDER


ROBERT A. MCCLATCHEY, Director
Atmospheric Sciences Division

This report has been reviewed by the ESD Public Affairs Office (PA) and is releasable to the National Technical Information Service (NTIS).

Qualified requestors may obtain additional copies from the Defense Technical Information Center. All others should apply to the National Technical Information Service.

If your address has changed, or if you wish to be removed from the mailing list, or if the addressee is no longer employed by your organization, please notify GP/IMA, Hanscom AFB, MA 01731. This will assist us in maintaining a current mailing list.

Do not return copies of this report unless contractual obligations or notices on a specific document requires that it be returned.

REPORT DOCUMENTATION PAGE			FORM NO. 104-100	
1. AGENCY USE ONLY (Leave blank)				
2. REPORT DATE 15 February 1991		3. REPORT TYPE AND DATES COVERED Scientific No. 3		
4. TITLE AND SUBTITLE Front Detection With Doppler Radar		5. FUNDING NUMBERS PE 637075 PR 2781 TA 01 WU AE Contract F19628-87-C-0124		
6. AUTHOR(S) Donald Hamann				
7. PERFORMING ORGANIZATION NAME(S) AND ADDRESS(ES) ST Systems Corporation 109 Massachusetts Ave. Lexington, MA 02173		8. PERFORMING ORGANIZATION REPORT NUMBER		
9. SPONSORING MONITORING AGENCY NAME(S) AND ADDRESS(ES) Phillips Laboratory Hanscom AFB, MA 01731-5000 Contract Manager: Kenneth Glover/LYR		10. SPONSORING MONITORING AGENCY REPORT NUMBER PL-TR-91-2034		
11. SUPPLEMENTARY NOTES				
12a. DISTRIBUTION AVAILABILITY STATEMENT Approved for public release; distribution unlimited		12b. DISTRIBUTION CODE		
13. ABSTRACT (Maximum 200 words) A technique to detect wind discontinuities associated with gust and synoptic fronts. It first transforms the Doppler velocity and reflectivity data into gradient vector fields by applying a series of templates to the data. From these vector fields, regions with large gradient magnitudes are isolated and edges or contours extracted where both the magnitude and direction information are used. A bi-directional search orthogonal to the local gradient vector is performed to extract lines of strong gradients. A multiplicity of somewhat parallel lines are often produced, with these being reduced to a single line through the selection of the most significant of these lines. The technique utilized in this study is a fast, efficient means of detecting large gradient regions in any two-dimensional field. It has been successfully applied to both Doppler velocity and reflectivity factor fields. It is shown that individual analyses of these two fields results in only partial detection of the feature. However, when they are combined into a single product, the result is a continuous depiction. This latter product is readily amendable for the application of a variety of forecast tools.				
14. SUBJECT TERMS Doppler radar, synoptic fronts, gust fronts, automated detection, NEXRAD		15. NUMBER OF PAGES 32		16. PRICE CODE
17. SECURITY CLASSIFICATION OF REPORT Unclassified	18. SECURITY CLASSIFICATION OF THIS PAGE Unclassified	19. SECURITY CLASSIFICATION OF ABSTRACT Unclassified	20. LIMITATION OF ABSTRACT Unlimited Distribution	

FOREWORD

This Scientific Report details the results of research performed by ST Systems Corporation (STX) under Contract F19628-87-C-0124 with the Atmospheric Sciences Division, Geophysics Laboratory.

Accession For		
NTIS	Special	<input checked="" type="checkbox"/>
DTIC TAB		
Unannounced		
Justification		
By		
Distribution		
Availability Code		
Avail and/or		
Dist	Special	
A-1		



FRONT DETECTION WITH DOPPLER RADAR

by
Donald J. Hamann
ST Systems Corporation (STX)
109 Massachusetts Ave.
Lexington, MA 02173

I. INTRODUCTION

An important task for the operational forecaster is the detection and monitoring of synoptic scale fronts. These meteorological features often have significant weather and wind shear associated with them that can adversely affect aircraft operations. Currently, the forecaster follows the progress of fronts by relying upon hourly observations from standard surface reporting stations and the even less frequent satellite observations. The resolution in space and time of these observations is less than optimum for NOWCASTing purposes and is often insufficient for the provision of guidance for many operations such as those associated with air terminals. Doppler radar provides a capability for detection of such fronts that other instrumentation is unable to provide. With the new WSR88D radar systems, data will be collected every 5 minutes with spatial resolutions of less than 2 km within 100 km and 4 km within 200 km of the radar.

The term front is usually applied to the low density edge of a density gradient in the atmosphere. The length of this discontinuity can be relatively short (a few to tens of kilometers) such as that produced by thunderstorm outflow or a seabreeze or can be long (100s of kilometers) as is often seen with synoptic scale warm and cold fronts. Because these are density discontinuities they are always in a pressure trough and so have wind direction and speed variations across them. The magnitude of the pressure trough and accompanying wind variations is related to the intensity of the density gradient.

Doppler radar measures radial velocities at discrete ranges along a radar beam when there is sufficient returned signal. As the beam scans in azimuth, data are collected at regular intervals (of the order of 1°), therefore providing an areal map of radial velocities. For air velocities to contribute to the measured radial velocity there must be a component along the radar beam.

The presence of scatterers in the form of precipitation or refractive index gradients may allow Doppler radar to detect the wind variations associated with fronts. Both the directional and magnitude shear that occur across fronts will contribute to gradients in the measured radial velocities. This report examines the potential of Doppler radar seeing the gradients associated with such fronts and presents a technique for their automatic detection.

II. TECHNIQUE DESCRIPTION

A. Overview

Doppler radar cannot measure the true wind field gradients across a front because it detects only one component of the air velocity, namely that along the radar beam. This radial velocity (V_R) is related to the east (u), north (v), and upward (W) components of the particle motions by the following expression:

$$V_R(r, \phi, \theta) = u \sin(\phi) \cos(\theta) + v \cos(\phi) \cos(\theta) + W \sin(\theta) \quad (1)$$

where ϕ and θ are the azimuth and elevation angles respectively.

W contains contributions from the vertical air velocity (w) and the fall velocity (V_T) of the scattering particles. When the radar beam is oriented along the air velocity vector, the radial velocity is an accurate estimate of the air velocity. However, when the beam is orthogonal to the wind the radial velocity goes to zero. As noted before, the velocities across the front vary in both magnitude and direction. The radar beam can be expected to be aligned along the local wind vector only in a few very isolated locations. With the beam scanning in azimuth, this means that the radial velocities and their gradients will vary as a function of aspect angle between the beam and the front. This dependability upon aspect angle plus the natural variability of the wind fields along a front makes the objective determination of the location of fronts a difficult task.

Real-time plan-view displays of radial velocity data often provide readily observable structures interpretable as fronts. These structures usually consist of elongated regions of strong gradients. Because they are discernable by the eye, it follows naturally that the task of automated detection might be viewed as an image analysis problem. Work in computer vision has already solved many image analysis objectives in areas such as robotics, medicine and astronomy. A principal motivation for using visual techniques to detect fronts lies in their ability to repre-

sent objects by their boundaries. These boundary representations can be later integrated into pattern recognition routines. This correlates well to the human visual system where studies have shown mammals to be adept at recognizing objects from crude outlines. Hubel and Wiesel (1979) suggest that the visual systems of mammals respond to edges of images and that this can be simulated with computer analysis by employing special template matching edge detectors.

B. Edge/Gradient Detection

The focus of this technique is the detection of lines of maximum gradients, which in image analysis is termed edge detection. This type of analysis is best performed after the radar data have been transformed to rectangular Cartesian space and gradients have been computed over the entire resultant image. Local image discontinuities are determined by identifying areas within a small spatial extent where the pixel intensities change rapidly. These regions are called edges. Operators which localize these edges compute the direction, which is aligned along the local pixel gradient, and a magnitude of the pixel intensity change. These two parameters are ideal in assembling boundary features. They define the vector oriented in the direction of the first derivative of the original field with a magnitude equal to that of the first derivative value. Focus on the large values of this field directs attention to abrupt changes in the derivatives like those seen in the velocity data at fronts or at the edges of precipitation areas. The vector directions are oriented orthogonal to the front. We, therefore, have a very good description of the location, orientation, and strength of the front. It should be noted that some parametric models are available that can describe more detailed local information than the two-parameter direction and magnitude vector. These methods, however, are much more computationally complex and are perhaps unnecessary in distinguishing large scale features.

III. TECHNIQUE IMPLEMENTATION

The adopted analysis technique involves the following procedures:

- Preprocessing to edit and transform the data from spherical to Cartesian coordinates.
- Computation of gradients, either velocity or reflectivity

- Extraction of "edges" based on gradient magnitudes and orientations.
- Association of "edges" into streaks (fronts) based on continuity.

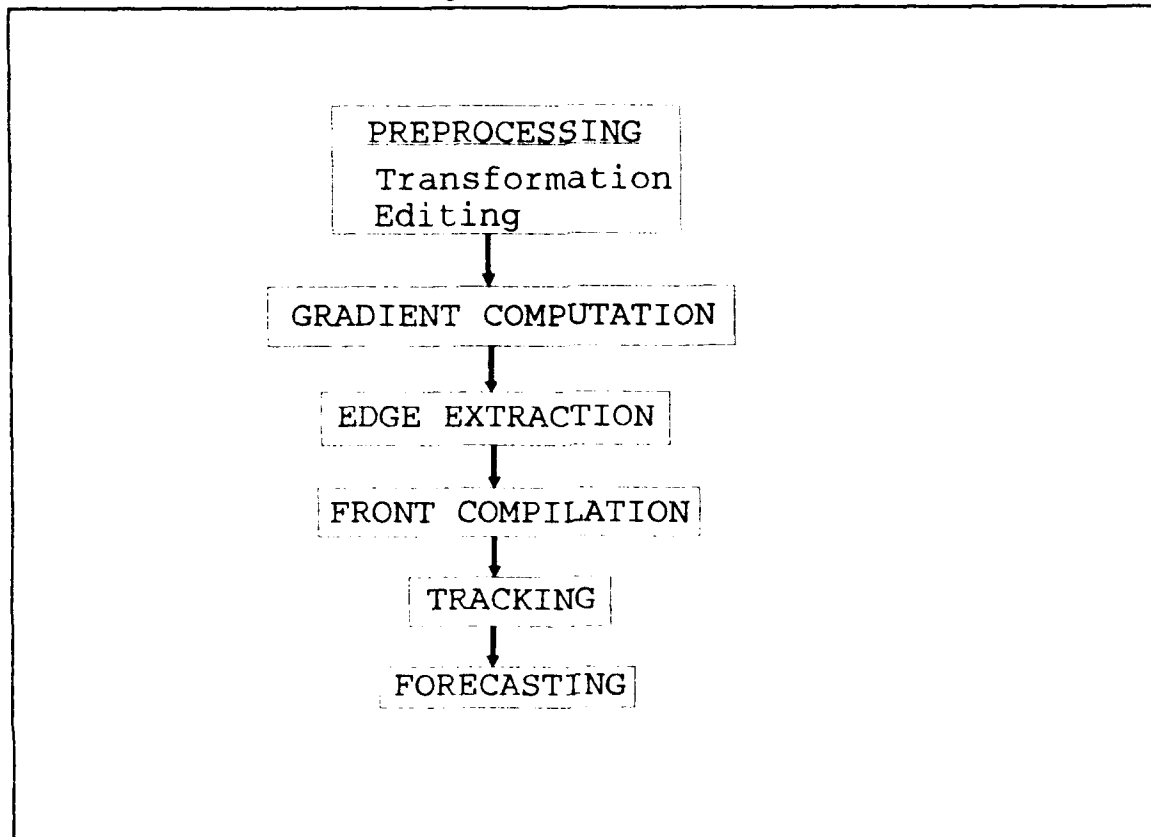


Figure 1 Flow Diagram for Front NOWCAST Generation

Once the fronts are detected correlations with previous times are required so that forecasts can be generated. The data flow for this processing is depicted in Fig. 1.

It should be noted though that the tracking and forecasting functions are not addressed in this report but are left for future exploration.

A. Preprocessing

Before gradients are computed, the radial velocity data are transformed to Cartesian coordinates and edited to remove spurious data and to dealias velocities as needed. The following sections will describe the procedures followed in each of these processes.

1. Coordinate Transformation

The use of image processing techniques requires the radar data to be converted from the spherical framework in which they were collected to a rectangular Cartesian format. Two methods were implemented for this conversion:

- A bilinear interpolation technique (BIT), designed to produce as exact an image as possible from the original data,
- A grid filling technique (GFT), developed to create images quickly, sacrificing some accuracy for speed.

While the greater accuracy of the first technique is, in general, preferred, the development of the second routine was necessitated by the performance limitations of the MicroVAX/GPX II computer used for this task. Evaluation of the responsiveness of the imaging routines is better performed using data from the more precise interpolation scheme. On the other hand, the faster technique allows the application of the technique to a time series and/or three dimensional analysis and therefore testing with a greater variety of data. Comparison of similar results from the two techniques allows the evaluation of the effects of the utilization of the two techniques.

a. The Bilinear Interpolation Technique, BIT

Mohr and Vaughan (1979) developed an efficient technique that accurately converts radar data from spherical to Cartesian coordinates. For each volume scan the Cartesian grid points are sorted to be consistent with the manner that the data are collected in each volume scan. This reduces the number of computations required and allows the processing of the data as they are ingested, thereby reducing the amount of required data storage. A constraint of BIT requires the radar data to be collected using a known constant elevation scan sequence. This scheme can be used to generate either vertical or horizontal planes. Vertical planes could prove to be useful in the better definition of sloping frontal boundaries.

b. The Grid Filling Technique, GFT

Cohan (1990) implemented a simple technique, the GFT, on the GL/LYR MicroVAX/GPX workstation to transform radar data to Cartesian grids for the generation of near real-time displays. The GFT iterates through the cells of each radial of radar data and assigns the data to the nearest

adjacent Cartesian grid point. Sometimes multiple data values are assigned to the same grid position. When that happens, the last data value assigned to the grid position is retained as the final value. The GFT involves a minimum of calculations but sacrifices some accuracy and has indeterminate effects upon the small scale fluctuations within the data.

2. Filtering

Because this technique requires good estimates of the first derivatives of the data, it is important that there is as little spurious data as possible. This preprocessing phase was introduced to remove noise and small scale features that would otherwise detract from isolating and identifying large scale wind discontinuities. A low-pass filter was selected to remove such features. Weights are applied to the data to compute a mean value for the central data point according to the formula

$$\overline{D}_i = \frac{\sum_{j=-N}^N [W_{i,j} D_{i,j}]}{\sum_{j=-N}^N W_{i,j}} \quad (2)$$

where D_i is the data value at the central grid point and $W_{i,j}$ is the weight applied to the $(i+j)$ th data point.

3. Dealiasing

Doppler radars can estimate velocities only within a specific dynamic range or Nyquist range, such as ± 35 m/s. Often the actual velocities are outside that range. The radar detects such motions by aliasing the true velocities into the Nyquist range deterministically. This results in extremely large artificial gradients that will provide problems in any automatic front extraction. As a result, velocity dealiasing, the process of replacing aliased velocities with their correct values, is extremely important for the success of this technique. Because of the complexity of automated dealiasing, this problem is left to others. Simplistic dealiasing techniques have been implemented and any features that appear in later analyses due to residual aliasing are removed from consideration.

B. Edge Detection

Once the data are interpolated and "cleaned," gradients can be calculated with templates. The abrupt change in gradients is then extracted using edge detection.

1. Template Application

The computation of gradients involves the use of multiple templates that contain weights to be applied to the data fields. These particular templates extract both directional and gradient information in a computationally efficient manner. The weights used in the template are based on the Kirsch operator (Kirsch 1971) which states that the gradient of an edge can be given by Eqn 3:

$$S(x) = \max[1, \max_k \sum_{k=1}^{k+1} |f(x_k) - f(x)|] \quad (3)$$

where $f(x_k)$ are the eight neighboring points and where subscripts are computed as modulo 8. The equivalent of this equation, which makes this method so attractive, can be made with four separate templates that are matched to the image. These templates have an odd number of elements whose values are structured to estimate both magnitude and direction (See Fig. 2 for example). Larger configurations may also be used but these will involve more templates and will, of course, be more costly to run.

The templates are implemented through the cumulative addition of data values added on the positive side of the template and subtracted on the negative side. The sums of these cumulative values are proportional to the strength of the local gradient along the axis of the template (the line oriented perpendicular to the line of 0s). The sign of this summed value specifies to which side of the template axis the gradient is oriented. This means that with four separate templates, the local gradients in eight directions can be determined. The template with the largest value is selected as that representing the true gradient magnitude and orientation. The magnitude of the gradient is determined from the summed values within the template and the direction is determined from the orientation of the template and the sign of the summed value. This procedure is applied to every data point within a plane and yields two resultant fields - magnitude and direction of the local gradients.

Due to lack of scatters, the radar does not usually provide a definition of all points within the plane to be analyzed. As a result, universal appli-

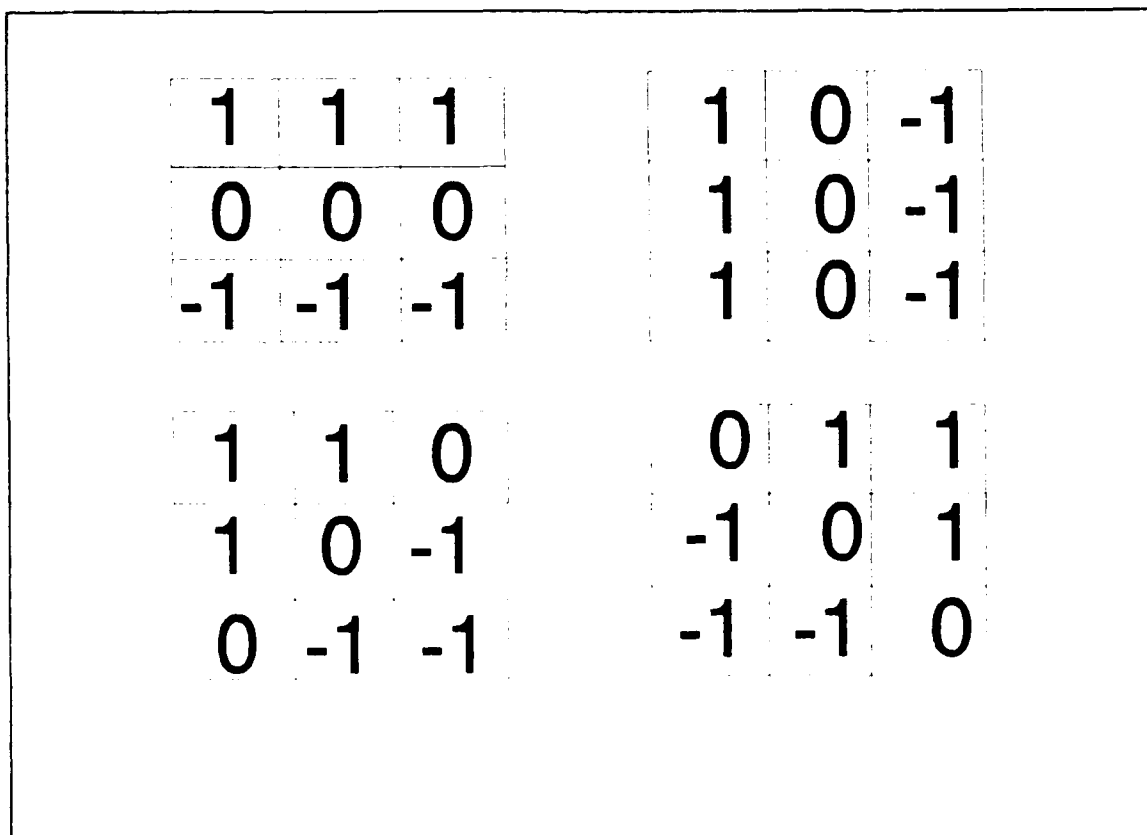


Figure 2 The four templates used for a 3 x 3 configuration.

cation of the templates results in maximum gradients being artificially skewed toward echo edges. This effect is more apparent in the velocity than reflectivity data. Therefore, a routine was required to handle any "holes" in the image. The most conservative approach would be to require all points within a template to be defined for the template to be used. This has the effect of ignoring gradients at the perimeter of echoes. Sometimes, this is where significant real gradients can occur, especially with reflectivity data. A more "relaxed" approach has been adopted where a monitoring function has been defined that ensures that the number of defined data points on each side of a template exceeds a user-specified threshold before gradients are computed. When this threshold is not realized, no gradient is computed for that point.

This monitoring function has been incorporated into the template routine itself. Concurrent to the summing of the data for each template, counters are tripped for each valid data point appearing on each side of the object point. If the threshold number of points (N_T) is attained on each of the positive and negative sides of the template, a local gradient magnitude and direction are computed. For each template of the group

of four, averages of the valid points (V_{ave+} and V_{ave-}) are computed and multiplied by the number of template array points (N_+ and N_- respectively). This latter step is taken because sums and not averages are used in subsequent analyses. The local gradient for that template is then computed by

$$\Delta \sum V = \sum V_+ - \sum V_- \quad (4)$$

If any one of the four templates fails the number threshold test, no gradients are retained for that particular object pixel.

C. Streak Determination

After the gradient magnitudes and directions are computed for all array points, the next step is to extract the most significant gradients. In image processing these features are called streaks. These streaks are the basis for frontal compilation.

1. Collecting Streaks

The magnitude and direction of the local discontinuities can be combined in a heuristic search to form sequences of elements or streaks. A buffer is created containing the computed magnitudes and associated directions for all pixels for which there is a valid gradient value. Contents of this buffer are then sorted with respect to the magnitudes of the gradients. The strongest value is chosen as the start point for the analysis, P_{S1} . A bidirectional search (described below) is performed about P_{S1} where the associated gradient direction is used to constrain search directions. Once the search is started in one direction, it is continued along the front edge of each successive element until no more successors are found. Then attention is focussed in the opposite direction from P_{S1} until all potential elements in that direction are found. A line (streak) joining these elements is generated if there are sufficient elements. Any elements used in a streak are constrained from use within any other.

The streak collection algorithm then selects the largest unused gradient magnitude as the initial point P_{S2} for the next streak. The construction of this second streak proceeds as with the first. This process then continues to select subsequent start points P_{Si} and associated streaks until all values in the gradient list are exhausted.

The search routine is a recursive algorithm that places the object pixel P_{Si} in an initially empty list for the i th streak and denotes it as "used" in the sorted gradient list. It then scans the three adjacent pixels in the direction associated with P_{Si} . Each pixel is then tested in turn to see if it has

been previously used and, if not, whether it meets a magnitude threshold. Each qualifier is then subjected to a weighting factor that is related to its magnitude and direction as compared with that of its adjacent predecessor. This ensures maximum directional continuity of the resultant streak. The valid neighboring pixel with the largest positive weighting value then becomes the object pixel and the process is repeated until a set of neighboring pixels fails to provide a qualifying successor. Then process is then repeated in the opposite direction from P_{Si} . When all the possible points are collected in that direction, a determination is made whether enough pixels were gathered to retain the streak. If the streak is not retained, the pixels collected in the list for that streak are reassigned as unused.

Several editing procedures for pruning and lengthening streaks to improve definition of primary boundaries remain to be implemented. The goal here is to produce a single line associated with each wind discontinuity and/or front that is observed in the radar data.

IV. ANALYSIS PRESENTATION

A. Implementation

All software is modular and user interactive. The imaging algorithms were written in the C programming language to take advantage of various memory allocation routines and to use variable bit data structures. Graphics software was written in Fortran code to allow the easy use of the Digital Equipment Corporation Graphic Kernel System (DEC GKS) resident software. As part of the interactive feature of this software package, there are several input parameters to define such things as filters, imaging templates, and graphic images.

B. Preprocessing Evaluation

It should be mentioned that examples presented in this section are taken from a single frontal passage episode. Although several cases were reviewed, it is believed that the notable features of this wind discontinuity detection algorithm can be described using this one example. The BIT technique was used to transform the data to Cartesian space. The spherical radar data were collected on November 16, 1989 by the GL/LYR 10 cm Doppler radar located in Sudbury, MA. The radar scanned in PPI mode, with 768 data cells per radial and approximately 400 radials per revolution.

1. Grid Resolution

Several considerations had to be made before applying the edge operator template to image. The first and most obvious was the selection of a grid resolution. The primary goal here is to ensure the most accurate representation of the data contained in the original radar data. Fig. 3 depicts a coarse resolution grid (2.5 km). The data appear blocky, but more importantly, fine scale details of the original data are lost and cannot be recovered. In fact, there is no discernible boundary. Figs. 4 and 5 contain successively finer grids, 1.0 and 0.64 km, respectively. The results become noisier with the decrease in grid spacing, but the finer scale structures are better represented. If needed, the noisiness can be reduced through the appropriate use of filters. The 0.64 km grid resolution provides an adequate degree of data coherence while maintaining a satisfactory level of machine performance.

2. Filter Characteristics

Often the interpolated data will need further smoothing or filtering. To fit such a need, a simple uniform, $n \times n$ low-pass filter was integrated into the code. Figs 6 and 7, where n is 5 and 9 respectively, depict the results of the application of a uniform filter to the image in Fig. 5. The 5×5 filter (Fig. 6) effectively dampens noise and results in better streak compilation. On the other hand, the 9×9 filter (Fig. 7) reduces the edge gradients to such an extent that streak extraction is less effective. This is because the boundaries are spread into the data-void regions. From these figures it is apparent that the filter size should be kept small to keep from significantly decreasing the sharp gradients.

Another test was performed where the 5×5 filter was applied three times successively to the data (Fig. 8). This multiple application of a small filter has a similar effect as the single application of the 9×9 filter (Fig. 5). Therefore, there is little advantage for gradient computations to applying a filter more than once to a data set.

C. Application of the Edge Template Operator

1. Template Size Considerations

The application of a template is analogous to the application of another filter in that it is effectively computing an average gradient over the area of the template. Therefore, the degree of averaging is a function of the

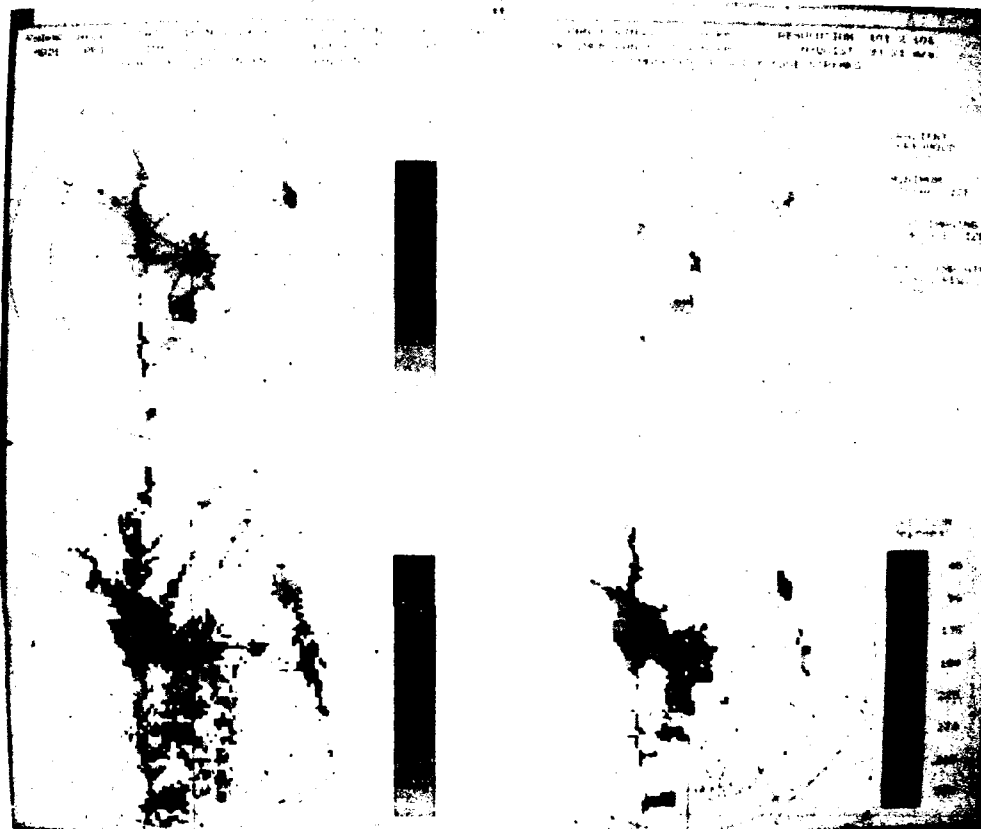


Fig. 3 Velocity image from 26 November 1989 collected at an elevation of 0.5° . Data have been interpolated onto a 101×101 grid with a 2.5 km grid spacing. Velocity data are presented in lower left frame, gradient magnitude in the upper left, gradient direction in the lower right, and streak construction in the upper right. No additional filtering has been applied. A 5×5 gradient template with at least 50 % of the template points being valid has been used.

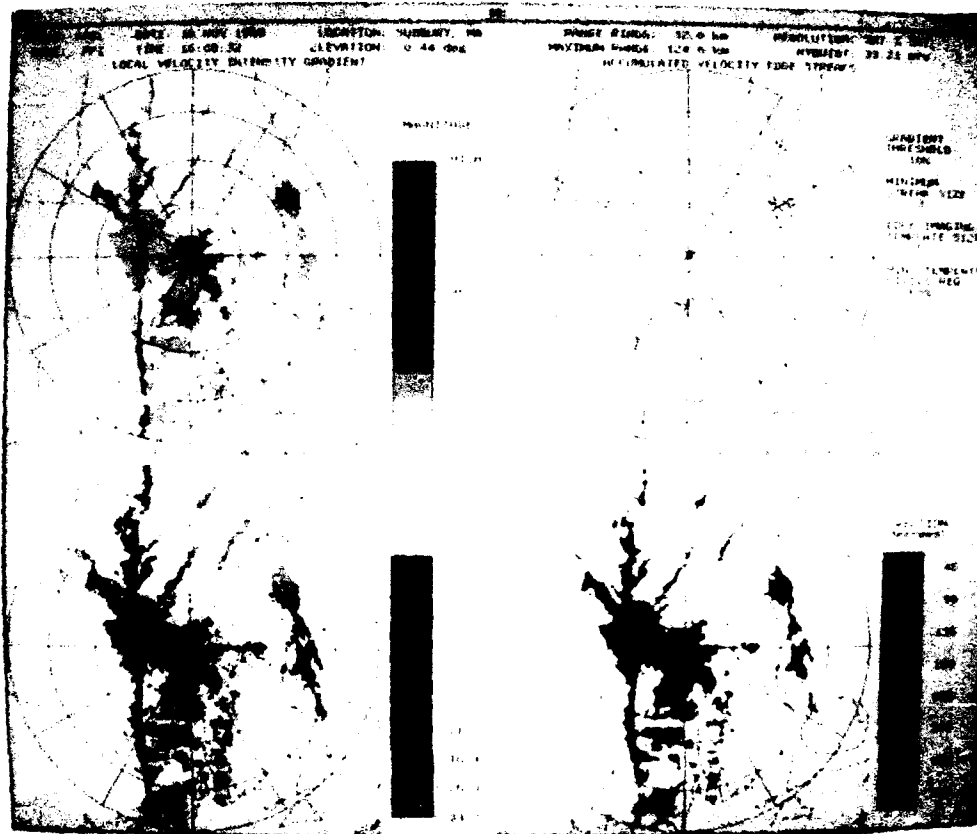


Fig. 5 Same as in Fig. 3 but with a 0.64 km grid spacing.

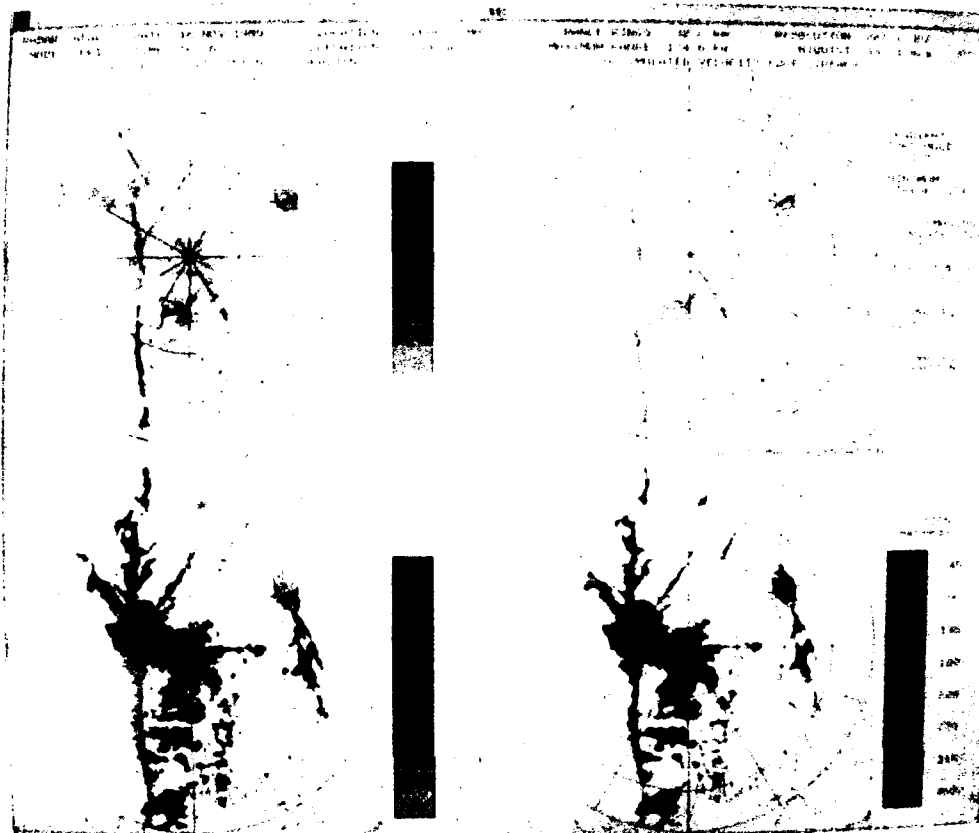


Fig. 6 Same as in Fig. 5 but where a 5 x 5 uniform filter has been applied.

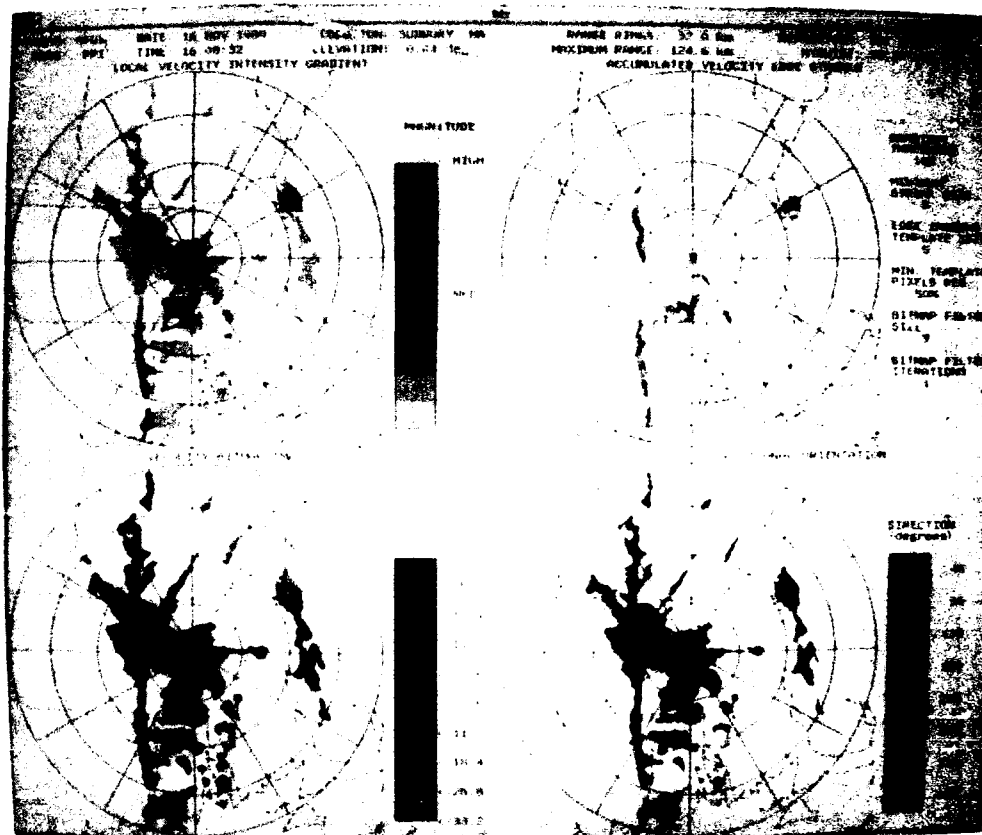


Fig. 7 Same as in Fig. 5 but where a 9 x 9 uniform filter has been applied.

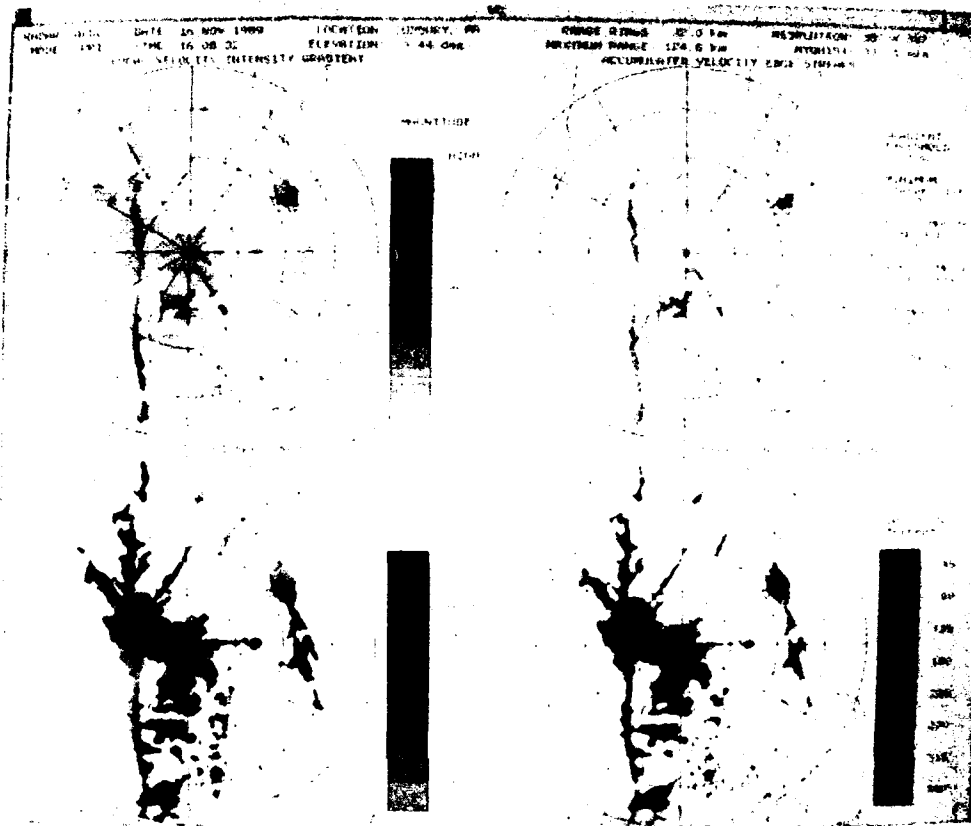


Fig. 8 Same as in Fig. 6 but where the filter has been applied three times.

size of the template, the larger the template, the more the averaging. It is therefore important to specify template size to be smaller than the scale of the high gradient regions. If template size is larger than that scale, the gradients will be underestimated. Also, if the template is of a size similar to the "noise" in the data, the resultant gradients will be noisy. Figs. 9 to 11 exhibit these effects. In Fig. 9, the small template size (3 x 3) obviously produces very noisy results. The level of noise diminishes as the template size increases (Figs. 10 and 11). The 7 x 7 filter of Fig. 10 appears to produce the best results in the derivative fields and in the resultant streak construction. As in the filter case, the larger template (Fig. 11) tends to wash out the gradients and make streak construction more difficult because it tends to blur the boundary features. This means that the size of the template should be no larger than is necessary to obtain useful results.

2. Data Void Considerations

As noted before, a technique was adopted to allow the application of the template near data void regions. This technique requires the monitoring of the number of valid data points within each template. If the number of points exceeds a threshold value, the template computation is accepted.

Figures 5, 12, and 13 depict the effects of varying the required percentages of valid data points within a template. In Fig. 5, 50% of data points within the template were required to be valid while in Fig. 12 all points must be valid. Comparison of the streaks for these two cases indicates that the more restrictive case results in less of the line being identified. For Fig 13, only one point on each side of the template was required for gradient values to be computed. While the line is well defined for this case, there are many more small scale features that would need to be removed for the analyses to be useful. It has been found that the minimum percentage of valid data points should be somewhat related to the data resolution, the degree of filtering, and the size of the template operator. For coarse resolutions and small templates, a high percentage is suggested. Conversely, for images that have been filtered considerably a smaller percentage appears appropriate as the data field has been massaged to become more uniform. This decreases the likelihood that a small sampling size would introduce errors in the determination of the local edge parameters.

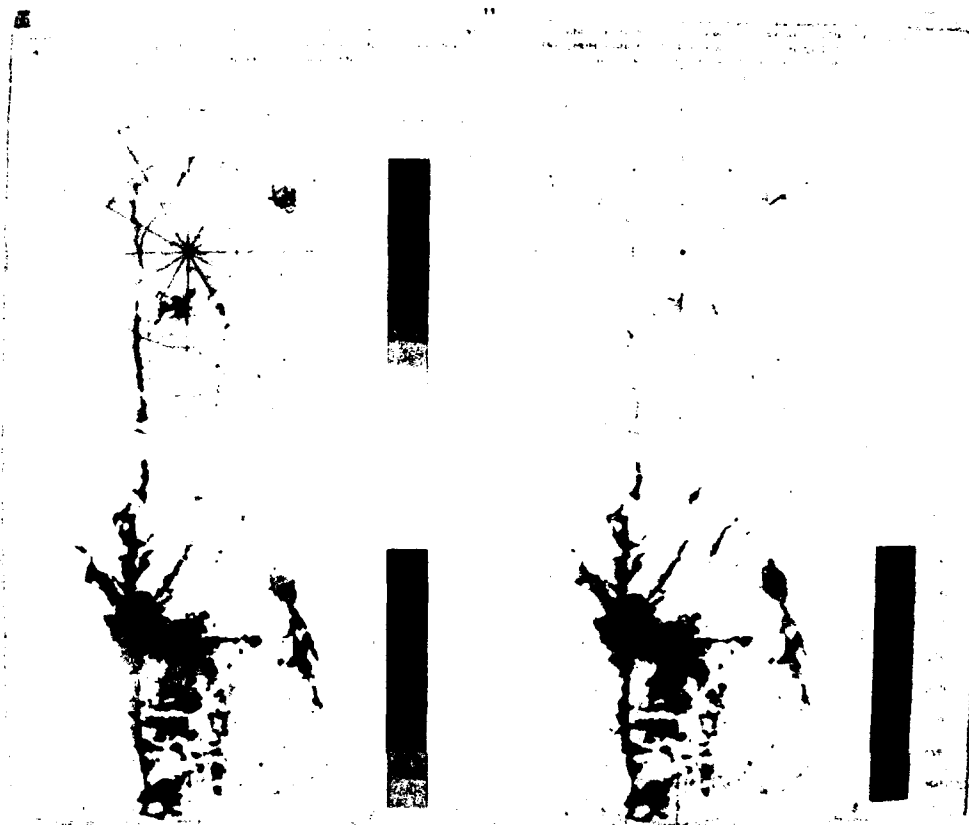


Fig. 9 Same as in Fig. 5 but where a 3 x 3 template has been used to compute the gradient magnitudes and directions.

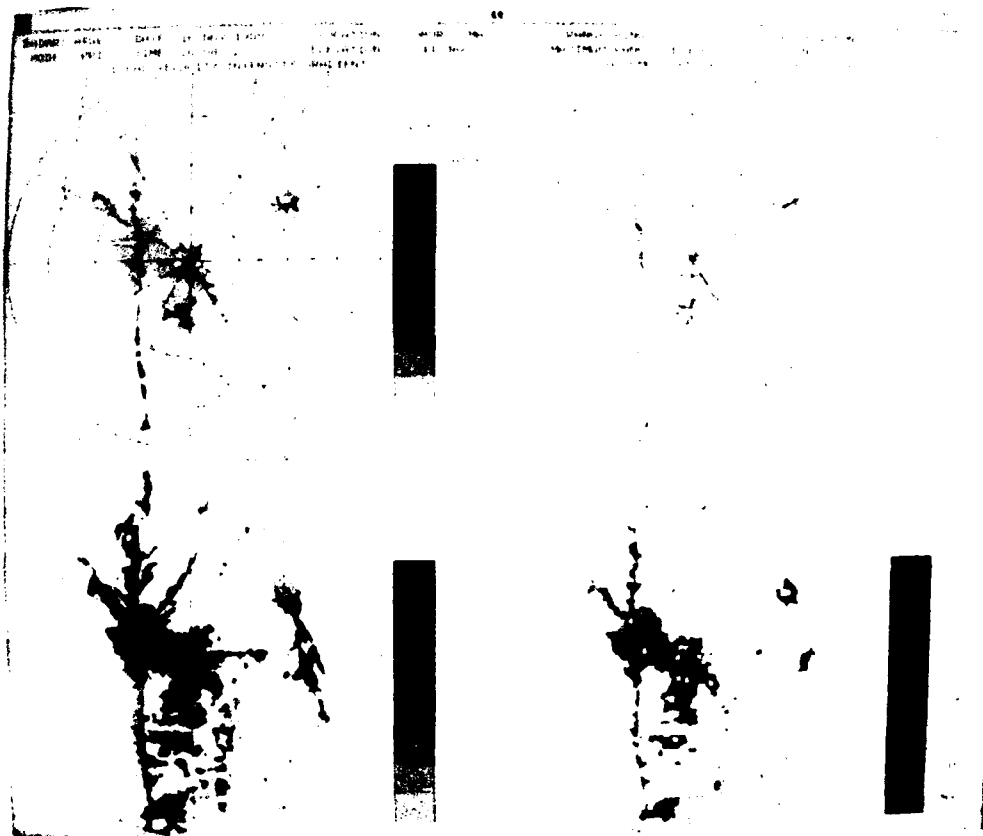


Fig. 10 Same as in Fig. 9 but where the template size is 7 x 7.

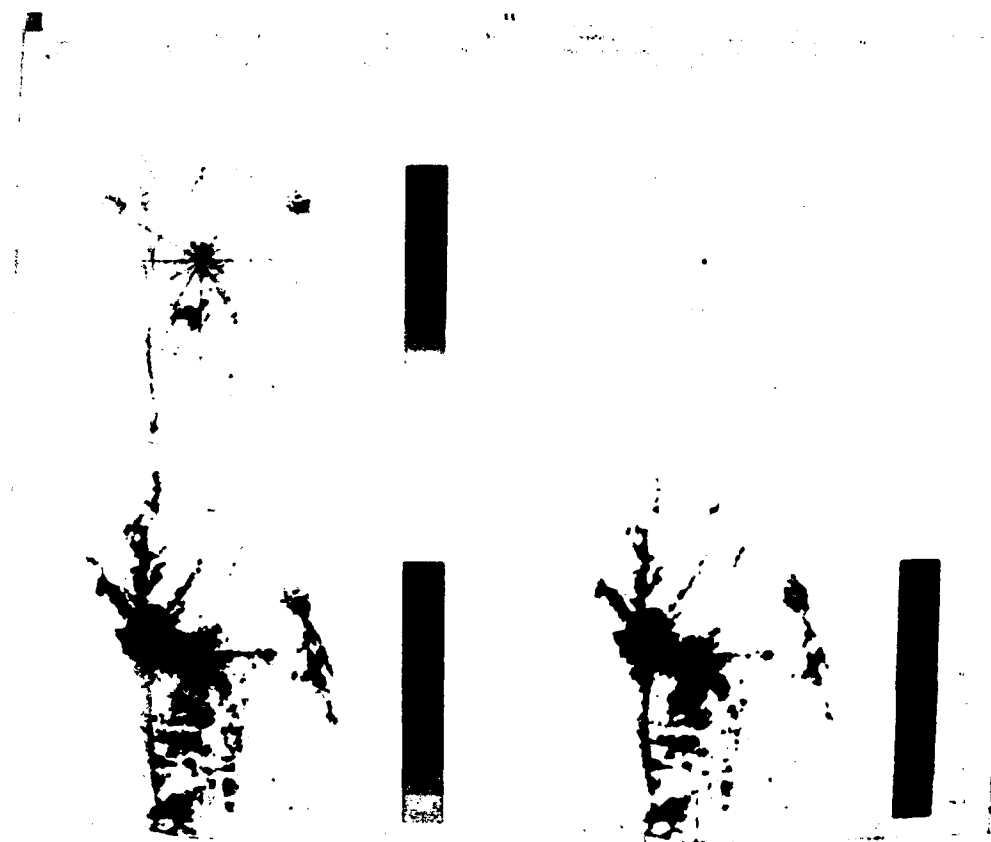


Fig. 11 Same as in Fig. 9 but where the template size is 11 x 11.

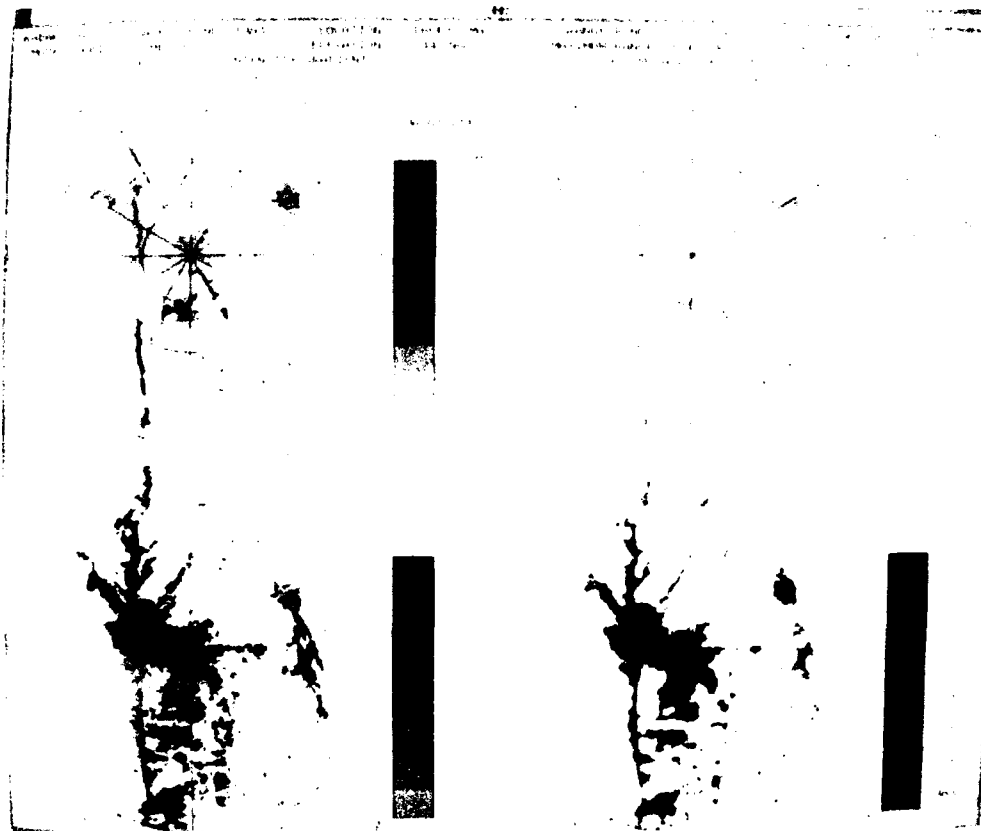


Fig. 12 Same as in Fig. 5 but where all data points within the template are required to be valid for gradient computations to be made.

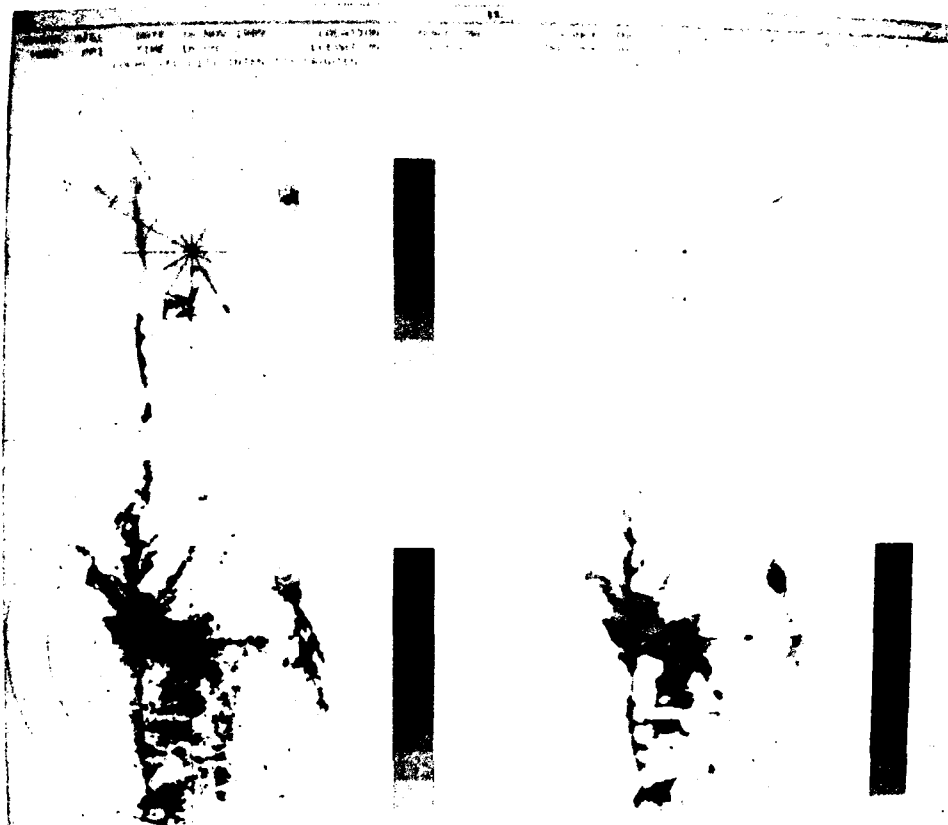


Fig. 13 Same as in Fig. 5 but where only one data point on each side of the template is required to be valid for gradient computations to be made.

D. Streak Line Association Constraints

Once the gradients are computed and arrays of magnitude and direction are compiled, the next step is to construct streaks. There are two major factors that could affect the performance of streak construction - acceptable gradient threshold and minimum acceptable streak length. These effects have yet to be tested. Currently the selection of thresholds by trial and error has produced adequate boundary streaks. Further investigation into this area is required.

E. Examples of Velocity Gradient Detection

Fig. 5 depicts the results of an application of the image processing routines on a radar Doppler velocity field. The edge detection operator clearly isolates the strong wind discontinuity in these data. The local orientation parameter image displays a predominant line along this feature. Also, there is a maximum in the magnitudes in an area that roughly coincides with that of the directional image. As mentioned before, because of velocity folding, additional regions of strong local change were produced. These false regions subsequently cause the streak assimilation routine to group incorrectly those areas and identify them as boundaries. Since velocity folding will generate extremely large local gradients, these areas will become the dominant zones in which the streak lines are formed. These detract from the otherwise favorable results from the directional parameter. This problem has been seen in all analyses for this date. While there are these spurious results, the routine does generate a distinguishable boundary along the edge of the front. Several breaks that appear along the front are, in part, an unfortunate result of the folding problem.

F. Examples of Reflectivity Edge Detection

The extraction of streak lines from reflectivity fields again was very successful, although not all lines were associated with the front, as one might expect. Again, the directional orientation parameter was well-behaved by producing a dominant local gradient line that tracks along the edge of the front. The magnitude parameter resulted in a contour line that outlined the stronger reflectivity echoes. As a result, the streak collection routine proceeded to assemble a boundary that essentially outlined a band of strong reflectivity. This can be seen in Fig. 14. Two lines are seen that bracket the perceived frontal line. Attempts have been made to integrate the reflectivity streaks with the velocity streaks. This required the development of an adjustment to the reflec-

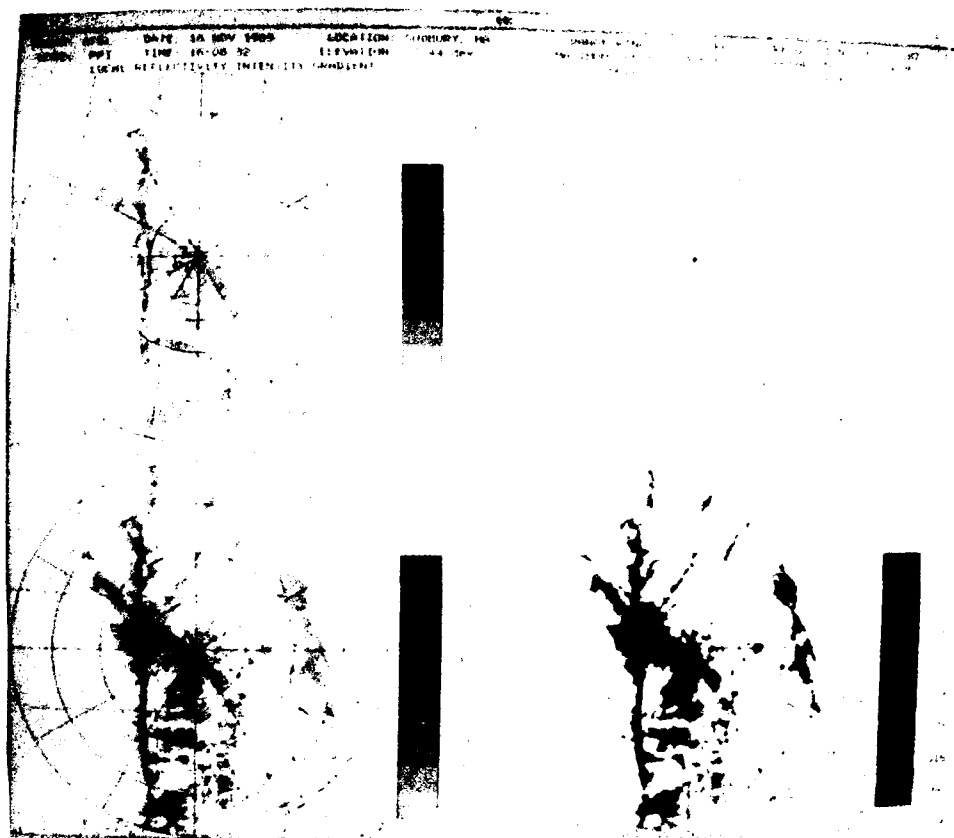


Fig. 14 Same as in Fig. 5 but for reflectivity factor data.

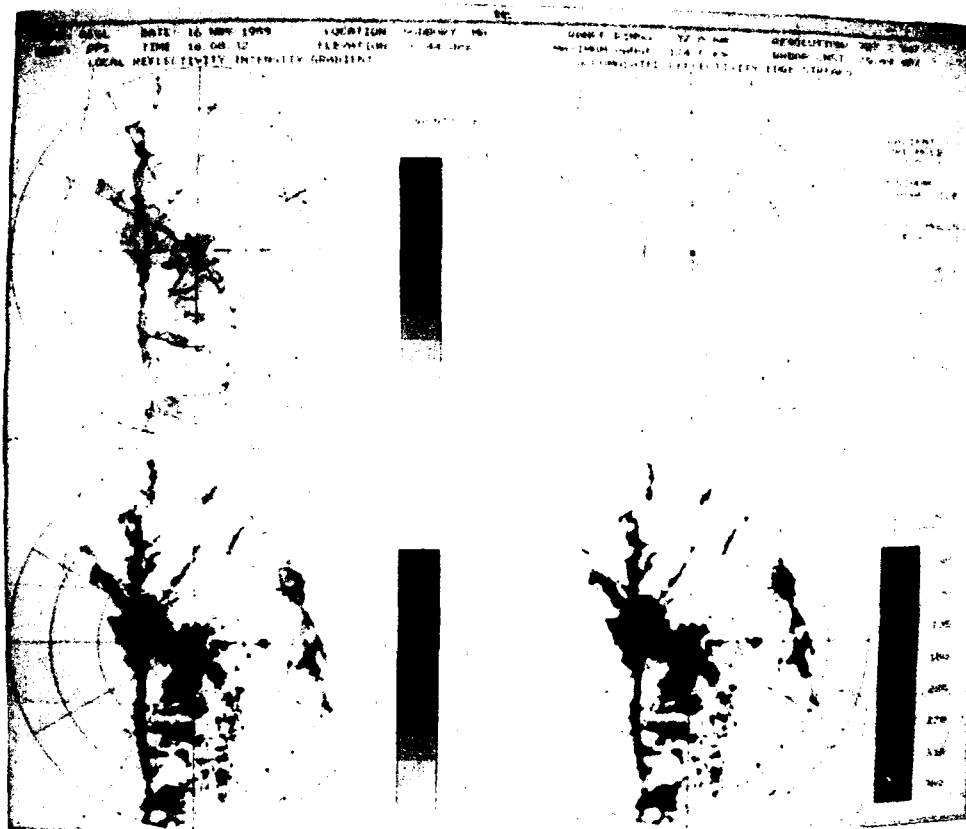


Fig. 15 Same as in Fig. 14 but where a 5 x 5 filter has been applied.

tivity streak collection procedure so that single boundary lines could be extracted. Instead of the streaks being assembled along the gradient magnitude lines, they are aligned along lines of high reflectivity intensities. Fig. 15 shows the image created under these guidelines. A distinctive primary boundary emerges along the front. Smaller features are also in evidence, possibly indicating ground clutter or the presence of small precipitation cells.

V. SUMMARY AND PROJECTION

The edge detection technique appears to offer an extremely promising method for isolating boundary areas. This technique can be applied to any image field but has been applied to radar reflectivity and radial velocity data. The detected boundaries in these fields may be associated with fronts or with the boundaries of precipitation. The information contained in the resultant fields can be used to monitor not only the locations but also gradient intensities. This latter aspect could yield information about changes in the intensity of the phenomenon with which the gradient is associated. This routine offers the ability to combine both reflectivity and velocity boundary information to improve detection of the complete boundary. Algorithms are available to combine multiple images to allow the derivation of a single boundary. Future work will entail evaluating the various parameters required for technique execution and for the combination of analyses from different fields and from multiple elevations. This latter effort could provide insight into the vertical structure of the front. The hope is to develop pattern recognition tools to derive sound predictions about the edge detected frontal boundaries.

VI. REFERENCES

- Cohan, M.D., 1990: User and Technical Manual for GL Weather Radar Displays. Report under Navy Cont. N0014-88-D-0333: Task 007.
- Hubel, D.H. and T.N. Wiesel, 1979: Brain mechanisms of vision. Scientific American, June 150-162.
- Kirsch, R.A., 1971: Computer determination of the constituent structure of biological images. Computers and Biomedical Research, 4, 315-328.
- Mohr, C.G. and R.L. Vaughan, 1979: An economical procedure for Cartesian interpolation and display of reflectivity in three-dimensional space. J. Appl. Meteor., 18, 661-670.